Journal of Physics: Conference Series **274** (2011) 012019 doi:10.1088/1742-6596/274/1/012019

Pulse processing in optical fibers using the temporal Radon-Wigner transform

L A Bulus-Rossini[1,2], P A Costanzo-Caso[1,2], R Duchowicz[1,2] and E E Sicre[3]

[1] Centro de Investigaciones Ópticas (CONICET La Plata – CIC), Camino Parque Centenario y 506, C.C. 3 (1897) La Plata, Argentina

[2] Facultad de Ingeniería, Universidad Nacional de La Plata, Calle 1 y 47, (B1900TAG) La Plata, Argentina

[3] Instituto de Tecnología, Facultad de Ingeniería y Ciencias Exactas, Universidad Argentina de la Empresa, Lima 717, (C1073AAO) Buenos Aires, Argentina

E-mail: lbulus@ing.unlp.edu.ar

Abstract. It is presented the use of the temporal Radon-Wigner transform (RWT), which is the squared modulus of the fractional Fourier transform (FRT) for a varying fractional order p, as a processing tool for pulses with FWHM of ps–tens of ps. For analysis purposes, the complete numerical generation of the RWT with $0 < p < 1$ is proposed to select a particular pulse shape related to a determined value of p. To this end, the amplitude and phase of the signal to be processed are obtained using a pulse characterization technique. To synthesize the processed pulse, the selected FRT irradiance is optically produced employing a photonic device that combines phase modulation and dispersive transmission. The practical implementation of this device involves a scaling factor that depends on the modulation and dispersive parameters. It is explored the variation of this factor in order to obtain an enhancement of the particular characteristic sought in the pulse to be synthesized. To illustrate the implementation of the proposed method, numerical simulations of its application to compress signals commonly found in fiber optic transmission systems, are performed. The examples presented consider chirped Gaussian pulses and pulses distorted by group velocity dispersion and self-phase modulation.

1. Introduction

The development of techniques for the analysis and synthesis of ultrashort optical pulses has become a relevant subject in many fields related with optical communications and photonic signal processing. From the spatial-temporal duality theory, well-known concepts and experiments developed in the framework of spatial image processing can be transferred to the temporal domain, providing new ways for analyzing and processing time optical signals [1]-[3]. Several applications were developed in connection with spectrum analyzers, pulse compression, and periodic pulse train formation with different repetition rates [4]-[11].

A generalization of the Fourier transform, i.e., the fractional Fourier transform (FRT) and the related Radon-Wigner transform (RWT), which have found many applications in several fields of spatial optical processing [12]-[15], have been recently applied to analyze dispersive pulse transmission [16]-[19]. Basically, the FRT of an optical signal can be also considered as a phase-space

signal representation where the fractional order p varies from zero (only time information) to one (pure spectral information). For the particular case of a periodic input signal, from the analysis of the complete RWT display it can be found the conditions for producing several periodic pulse trains having different duty-cycles and repetition rates [7], [8]. In this paper we propose to extend the RWT approach for pulse compression applications in cases where the input signal to be processed may be unknown. In this situation, the implementation of a photonic device to obtain a complete RWT display is very unpractical as it would require the use of a dispersive element and a quadratic phase modulator with a continuous variation and fine tuning of both, the dispersion parameter and the modulation coefficient to produce the suitable change of p along the desired range. To address this problem we propose a different approach that starts by applying a pulse recovery method. Many techniques have been developed in recent years for pulse characterization [20]-[24]. Here we employ a pulse recovery method based on the information obtained from two temporal intensity recordings of the pulse propagated through media with opposite signs, second order dispersion coefficients. Once the amplitude and phase information of the signal to be analyzed is recovered, the complete RWT for $0 < p < 1$ can be numerically produced. From this RWT display an adequate value of p required to process the pulse can be obtained. Finally, the selected FRT irradiance is synthesized by means of a photonic device combining quadratic phase modulation and second order dispersive transmission. Considering that the practical implementation of this device includes a scaling factor that depends on the device parameters, it is analyzed how the variation of its value can produce an enhancement of the particular characteristic searched in the processed pulse. The method is illustrated with applications concerning with pulse transmission by an optical fiber link affected with source chirping, third-order dispersion (TOD) and self-phase modulation (SPM).

2. Temporal RWT production

In the spatial domain, the squared modulus of the FRT associated with an optical signal $u_0(x)$, which is denoted as $|u_p(x)|^2$, can be obtained by performing a phase-space rotation of the Wigner distribution function (WDF) of $u_0(x)$ by an angle $\phi = p\pi/2$ together with a spatial frequency projection [15]. As this action also represent the Radon transform of the signal (which is of interest in tomography), the complete display of $|u_p(x)|^2$ for a varying fractional order $0 \le p \le 1$ becomes the RWT of $u_0(x)$. By using the spatial-temporal duality [1], [2], it can easily be obtained an optical device for producing a time-varying signal proportional to $|u_p(t)|^2$, which is shown in Fig. 1. An electro-optic phase modulator (EOPM) fed with a sinusoidal function of angular frequency ω_m is used together with a dispersion line having a second-order dispersion parameter Φ_{20}. This last component can be implemented using one or several linearly chirped fiber Bragg gratings (LCFG). The phase modulation is considered as $\phi_{20}\, t^2/2$ by using the parabolic approximation of the sinusoidal modulation waveform, which means that the quadratic phase factor becomes $\phi_{20} = \pm\theta_0\, \omega_m^2$ provided $\omega_m^2 T^2 << 1$, being T the pulse width and θ_0 the modulation amplitude. The sign of ϕ_{20} depends on whether the cosine modulation signal has a phase shift of π or 0 with respect to the pulse. The output optical power of this device becomes $P_{out}(t) = |u_p(t)|^2$, whenever the following relationships are satisfied [13]:

$$\phi_{20} = \frac{2\pi}{\lambda\sigma_0}\tan\left(\frac{p\pi}{4}\right), \tag{1a}$$

$$\Phi_{20} = \frac{\lambda\sigma_0}{2\pi}\sin\left(\frac{p\pi}{2}\right), \tag{1b}$$

being λ the mean wavelength and σ_0 a scaling factor with dimensions of $ps^2/(nm{\cdot}rad)$. It is to be noted that an additional quadratic phase modulation would be required for producing the amplitude FRT. However, since we are only interested in the square modulus of the FRT this second phase modulator is discarded in the device sketched in Fig. 1.

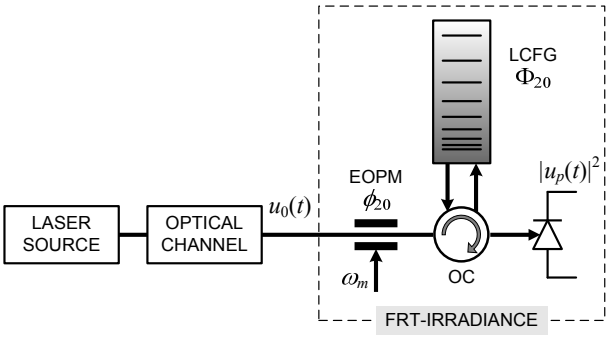

Figure 1. Photonic device for producing the FRT irradiance. EOPM: Electro-optic sinusoidal phase modulator having a quadratic phase factor $\phi_{20} = \pm\theta_0\,\omega_m{}^2$. LCFG: Linearly chirped fiber grating having a second order dispersion parameter Φ_{20}. OC: Optical circulator.

Thus, a synthesis operation can be carried out in a relatively simple way as only a particular value of p is to be selected. Nevertheless, the complete RWT optical production which is needed for signal analysis purposes becomes very troublesome as it would require a continuous, very precise variation of the device parameters accordingly with Eqs. (1). By this reason, a more convenient approach is to perform a numerical implementation of $|u_p(t)|^2$, for $0 \le p \le 1$. Once a particular value $p = p_C$ is chosen from the computer generated RWT display, this unique FRT can be optically produced using Eqs. (1) for selecting the device parameters. Of course, this approach implies to know the amplitude and phase information of $u_0(t)$, which is not the case in most applications. We next discuss the use of a recovery method for obtaining both, the amplitude and phase of $u_0(t)$.

3. Signal recovery method

We now discuss the procedure for recovering $u_0(t)$ when it becomes the unknown output signal of an optical channel acting as a "black-box". The first step to be done is to get the phase distribution of $u_0(t)$. To this end, we use a method based on the detection of two temporal intensities which can be considered the temporal domain analogue of a spectral approach proposed by C. Dorrer et al. [24]. It is based on the relationship that exists between the first order moment of the WDF and the instantaneous frequency $\nu(t)$ (or first order derivative of the phase). For a given signal, described by its complex envelope representation $u_0(t) = |u_0(t)| \exp(j\varphi(t))$, it can be demonstrated that

$$\int_{-\infty}^{+\infty} \omega\, W_{u_0}(t,\omega)\, d\omega = \frac{\partial \varphi(t)}{\partial t} |u_0(t)|^2 , \tag{2}$$

being $W_{u_0}(t,\omega)$ the WDF associated to $u_0(t)$ defined as

$$W_{u_0}(t,\omega) = \int_{-\infty}^{+\infty} u_0(t+\tau/2)\, u_0^*(t-\tau/2)\, e^{-j\omega\tau} d\tau = \frac{1}{2\pi} \int_{-\infty}^{+\infty} U_0(\omega+\omega'/2)\, U_0^*(\omega-\omega'/2)\, e^{-j\omega' t} d\omega' , \tag{3}$$

where $U_0(\omega)$ means the Fourier transform of $u_0(t)$. The WDF associated to a signal $u_f(t)$ whose spectral phase has been quadratically modulated is equal to the WDF associated to the original signal $u_0(t)$, affected by a temporal shear. This property is expressed as

$$W_{u_f}(t,\omega) = W_{u_0}(t - \Phi_{20}^r \omega, \omega) , \tag{4}$$

where W_{u_0} and W_{u_f} are the WDF's associated to the original and the filtered signals, respectively, being $-\tfrac{1}{2}\Phi_{20}^r \omega^2$ the spectral modulation signal. The temporal intensity of the modulated signal can be written in terms of its associated WDF as

$$I_{u_f}(t) = \left|u_f(t)\right|^2 = \int_{-\infty}^{+\infty} W_{u_f}(t,\omega)\, d\omega = \int_{-\infty}^{+\infty} W_{u_0}(t - \Phi_{20}^r \omega, \omega)\, d\omega . \tag{5}$$

By differentiating (5) with respect to the modulation coefficient it results

$$\frac{\partial I_{u_f}(t)}{\partial \Phi_{20}^r} = \int_{-\infty}^{+\infty} \frac{\partial}{\partial \Phi_{20}^r} W_{u_0}(t - \Phi_{20}^r \omega, \omega)\, d\omega \,. \tag{6}$$

By introducing the variable change $t' = t - \Phi_{20}^r \omega$ in (6), it turns into

$$\frac{\partial I_{u_f}(t)}{\partial \Phi_{20}^r} = \int_{-\infty}^{+\infty} \left(\frac{\partial W_{u_0}}{\partial t'} \frac{\partial t'}{\partial \Phi_{20}^r} + \frac{\partial W_{u_0}}{\partial \omega} \frac{\partial \omega}{\partial \Phi_{20}^r} \right) d\omega = \int_{-\infty}^{+\infty} \frac{\partial W_{u_0}}{\partial t'}(-\omega)\, d\omega \,. \tag{7}$$

Now, by taking into account that the variations of the WDF with respect to the sheared temporal axis t' are the same as the ones with respect to the original temporal axis t, i.e. $\partial W_{u_0}/\partial t' = (\partial W_{u_0}/\partial t)\,(\partial t/\partial t') = \partial W_{u_0}/\partial t$, Eq. (7) can be rewritten as $\partial I_{u_f}(t)/\partial \Phi_{20}^r = -(\partial/\partial t)\int_{-\infty}^{+\infty} \omega\, W_{u_0}(t,\omega)\, d\omega$. By replacing (2) into this last expression, it yields

$$\frac{\partial I_{u_f}(t)}{\partial \Phi_{20}^r} = -\frac{\partial}{\partial t}\left(I_{u_0}(t) \frac{\partial \varphi(t)}{\partial t} \right). \tag{8}$$

Equation (8), sometimes referred to as the temporal transport-of-intensity equation, has been used to measure temporal phase shifts induced by self-phase modulation or cross-phase modulation [25]. By using (8) it is possible to recover the phase of a given signal. Nevertheless, in order to obtain a feasible and easily attainable procedure, some approximations should be made. First, the derivative with respect to the modulation coefficient can be replaced by a centered finite difference approximation as

$$\frac{\partial I_{u_f}(t)}{\partial \Phi_{20}^r} \cong \frac{I_{u_f}(t)\Big|_{\Phi_{20}^r} - I_{u_f}(t)\Big|_{-\Phi_{20}^r}}{2\Phi_{20}^r} \,. \tag{9}$$

The quadratic spectral phase modulation can be produced by transmission of the signal through an optical fiber or by reflection in a LCFG, being Φ_{20}^r the second order dispersion coefficient of either device at the central angular frequency ω_0. In this manner, the temporal intensity derivative can be implemented by two temporal detections of the signal, each one affected by the same amount of second order dispersion, but having opposite signs. Taking advantage of this implementation, the intensity $I_{u_0}(t)$ can be approximated by the average of the two detections of the dispersed signal as

$$I_{u_0}(t) \cong \frac{I_{u_f}(t)\Big|_{\Phi_{20}^r} + I_{u_f}(t)\Big|_{-\Phi_{20}^r}}{2} \,. \tag{10}$$

It is worth noting that Eqs. (9) and (10) are only valid whenever the second order dispersion coefficient Φ_{20}^r remains small. Thus, in order to find the restrictions for Φ_{20}^r, lets consider a pulse with temporal and spectral widths Δt and $\Delta\omega$, respectively, being both symmetrical in a first approach. Since Φ_{20}^r is equal to the tangent of the shearing angle, it can be easily shown that the second order dispersion coefficient should be much lower than the ratio of the temporal width to the spectral width, i.e., $\Phi_{20}^r << \Delta t / \Delta\omega$.

Figure 2 shows a schematic diagram of the system proposed for recovering the phase of a signal. The input pulse $u_0(t)$ is split in two signals by the left 50/50 coupler. One pulse, after propagation through the left circulator (OC_1), reflection from the left side of the LCFG and again circulated by OC_1 is detected after passing the right 50/50 coupler. The second pulse, after being delayed a time T longer than the pulse width and circulated by OC_2, experiments a second order dispersion of opposite sign, since it is reflected from the right side of the LCFG. Thus, after two consecutive detections, the phase of $u_0(t)$ can be recovered employing Eqs. (8), (9) and (10).

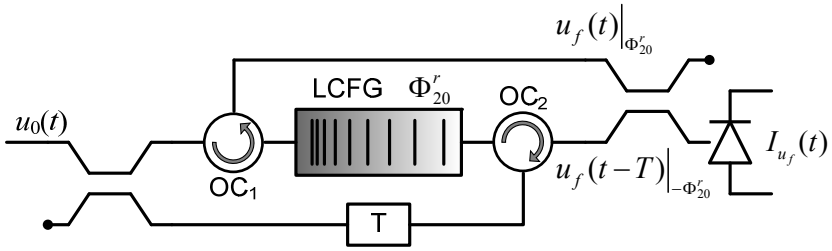

Figure 2. Schematic diagram of an implementation of the phase recovery device. LCFG: Linearly chirped fiber grating having a second order dispersion parameter Φ^r_{20}. OC$_1$ and OC$_2$: Optical circulators.

4. Implementation of a selected condition

In this section it is discussed the role of the scaling parameter σ_0 on the pulse processing operation since variations of σ_0 also produce changes in the RWT display. The value of this parameter is needed to obtain a practical optical implementation of the system; i.e., when the synthesis operation for producing the processed pulse is to be performed. However, by selecting an adequate value of this parameter when the RWT display is numerically produced, the shape of the pulse with the searched particular characteristic (found at the fractional order p_C) can be enhanced. By this reason, it is important to further analyze this point in connection with a practical optical realization. Thus, once the pulse to be processed is recovered employing the technique described in Sec. 3, several RWT displays can be computationally generated by varying the value of the scaling parameter in such a way that a proper selection of the σ_0 allows to find the fractional order p_C that best fulfills the desired processing conditions. However, there is a practical limit imposed by the parameters involved in the photonic device of Fig. 1 that is used to synthesize the selected FRT irradiance. Changes in the value of σ_0 are directly proportional to the value of the second-order dispersion parameter Φ_{20} and inversely proportional to the phase modulation parameter ϕ_{20} (see Eqs. (1a) and (1b)). Taking into account that it becomes more difficult to produce a wide range of ϕ_{20} values than a large second-order dispersion parameter variation, the attention will be focused on generating different values of σ_0 with feasible values of the phase modulation parameter.

In order to illustrate the procedure we consider the compression of a Gaussian chirped pulse (RMS width $T_0 = 10$ ps, $C = -6$ and mean wavelength $\lambda_0 = 1550$ nm), which is first recovered by applying the method of Sec. 3 by selecting $\Phi^r_{20} = 1.6\,\text{ps}^2$ ($\Delta t / \Delta\omega = 16.7\text{ ps} / (2\pi 160\,\text{GHz}) = 16.7\,\text{ps}^2$), a SNR = 14 dB and an irradiance recording average $N = 1000$. Since we are interested in selecting a compressed pulse from different RWT displays (by varying σ_0), it will be made a comparison between the curves consisting of the peak values of the FRT for each fractional order p. Such kind of graph can be regarded as "watching" the RWT display from the side of the fractional order axis and joining the highest values obtained for each p. Figure 3(a) shows these parametric curve for four different values of σ_0: –0.05, –0.1, –0.2 and –0.5 ps^2/(nm·rad). It is to be noted that not only the critical p that produce the largest intensity value changes, but also the peak value does. The highest intensity is obtained when the scaling factor is the smallest (in magnitude) of the four. In Fig. 3(b) it is shown the frequency of the modulation signal fed to the EOPM, when the modulation amplitude is $\theta_0 = 1$ rad. For the smallest value of σ_0, the selected p to achieve maximum compression is 0.647, and the modulation frequency is $f_m = 33.8$ GHz, while $p = 0.417$ and $f_m = 18.7$ GHz, when $\sigma_0 = -0.1$ ps^2/(nm·rad). Modifying the scaling factor in a wide range could lead to non-feasible practical implementation of the device. Nevertheless, selecting a more conservative σ_0 can still yield an enhancement in the processing of the pulse. A similar situation appears when considering θ_0 for a fixed frequency of $f_m = 10$ GHz which is shown in Fig. 3(c). The modulation amplitude values changes from 11.4 rad to 3.49 rad for a scaling factor of –0.05 ps^2/(nm·rad) and –0.1 ps^2/(nm·rad), respectively.

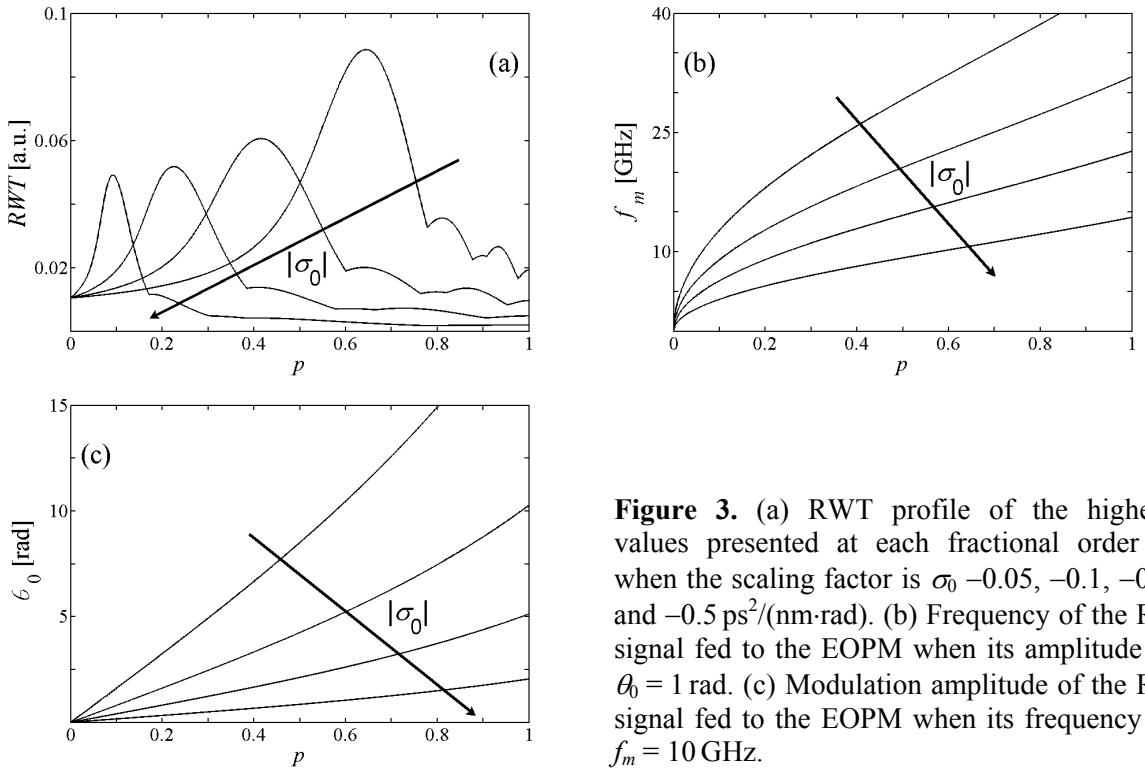

Figure 3. (a) RWT profile of the highest values presented at each fractional order p when the scaling factor is σ_0 −0.05, −0.1, −0.2 and −0.5 ps^2/(nm·rad). (b) Frequency of the RF signal fed to the EOPM when its amplitude is $\theta_0 = 1$ rad. (c) Modulation amplitude of the RF signal fed to the EOPM when its frequency is $f_m = 10$ GHz.

5. Signal analysis using the RWT

When the signal $u_0(t)$ gives rise to a RWT having a closed analytical expression, some simple relationships related with pulse compression can be established, e.g., if $u_0(t)$ is the output of a pulsed laser having a Gaussian amplitude envelope and linear chirp parameter C, or if the same pulse is transmitted through a certain length of standard optical fiber when dispersion effects up to the second order are considered [26]. In the more general case, when the shape of the pulse to be processed becomes more intricate the numerical generation of the RWT can not be avoided.

Before illustrating the pulse processing method with some examples, an important consideration regarding the RWT generation should be made. In order to mitigate the detection noise inherent to the recording process, several temporal intensities are averaged before applying the recovery method. As a consequence, the recovered pulse irradiance has a noise floor equal to the detection noise variance. This component, together with the amplitude and phase variations, contributes to the degradation of the numerically generated RWT. The noise floor produces an energy concentration around the origin for fractional order values near 1. For high SNR values (i.e., generally above 26 dB), it may be disregarded when producing the RWT display. But if low SNR values are considered, the recovered pulse waveform should be processed to reduce this effect before generating the RWT. To address this problem, we multiply the recovered pulse by a proper-sized window function to select the part where the modulus is greater than the noise floor. This approach extends the range of the method for SNR values below 26 dB allowing the selection of the adequate fractional order needed for pulse processing, especially when p_C falls above ~0.7. This situation is to be found in the following examples.

When the input signal $u_0(t)$ is a waveform associated with pulses suffering from high order dispersion or nonlinearities its RWT has not an analytical closed form, not being possible in these cases to obtain a simple expression of the optimum fractional order p_C which symmetrize and/or compress the pulse. In these situations, the information of p_C should be obtained from the RWT displays. As a first application, we select the signal $u_0(t)$ as an unchirped Gaussian pulse of initial

RMS width $T_0 = 5$ ps transmitted through a non-zero dispersion-shifted (NZ-DS) fiber link a distance large enough to be distorted by third order dispersion; i.e., $L = 3.6 \times L_{D3}$ (being $L_{D3} = T_0^3/|\beta_3|$ the third-order dispersion length). Besides, as a result of a dispersion compensation scheme, it is affected of a small amount of residual second order dispersion. The pulse is recovered employing the same value of second order dispersion parameter, $\Phi_{20}^r = 1.6\,\text{ps}^2$, since in this case $\Delta t / \Delta\omega = 12.8\text{ ps} / (2\pi 51.5\,\text{GHz}) = 39.6\,\text{ps}^2$. In Fig. 4 we compare three different the RWT's considering scaling parameters of –0.1, –0.15 and $-0.2\,\text{ps}^2/(\text{nm}\cdot\text{rad})$, in (a), (b) and (c), respectively, when the original pulse is recovered with a SNR = 23 dB and an irradiance recording average of $N = 1000$. Although the three RWT displays are similar and present fluctuations (due to intensity and phase errors) for high values of p, the compression/symmetrization effect changes substantially from one RWT display to the other, and it appears at different fractional orders p_C. From the inspection of each RWT display a symmetrized pulse presenting maximum compression is observed at $p_C = 0.91$, 0.86 and 0.79 for the RWT displays in (a), (b) and (c), respectively. The optical power of the processed pulse is shown for the three cases in Fig. 4(d). As it can be seen from these graphs, the best reshaped/compressed pulse is obtained with $\sigma_0 = -0.1\,\text{ps}^2/(\text{nm}\cdot\text{rad})$. The device parameters needed to synthesize the selected FRT ($p_C = 0.91$) become $\phi_{20} = -3.52\times10^{22}\,\text{Hz}^2$ and $\Phi_{20} = -24.4\,\text{ps}^2$ (i.e., $L \cong 1.18$ km of standard fiber optic or an equivalent LCFG). To produce the modulation coefficient, the RF signal needs to be a cosine with amplitude $\theta_0 = 5$ rad and frequency $f_m = 13.3$ GHz in phase with respect to the pulse.

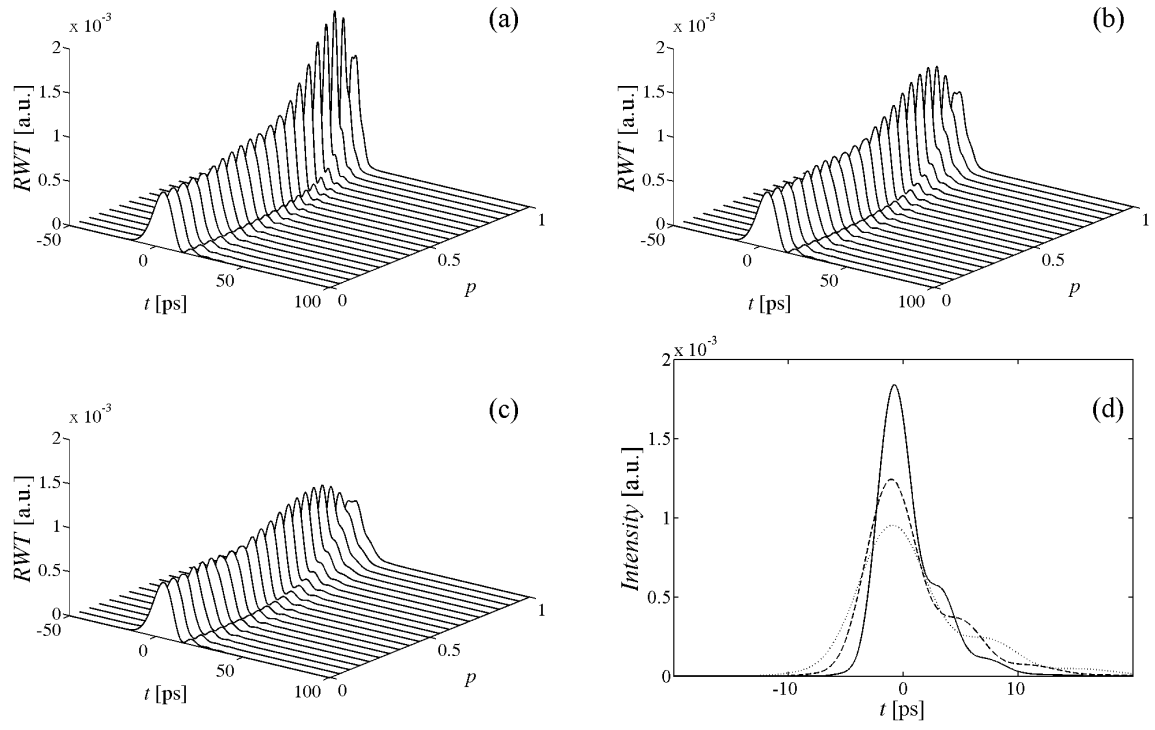

Figure 4. Processing of an unchirped Gaussian pulse with $T_0 = 5$ ps transmitted through a dispersion compensated optical fiber link that introduce TOD and a small amount of residual second order dispersion. In (a), (b) and (c) the RWT displays of the pulse recovered with a SNR of 23 dB, considering scaling factors of –0.1, –0.15 and $-0.2\,\text{ps}^2/(\text{nm}\cdot\text{rad})$, respectively; and in (d), the FRT irradiance of the processed pulses for the selected $p = p_C$ of each corresponding RWT in solid (a), dashed (b) and dotted (c) line.

Next, we consider the case of a pulse mainly affected by nonlinear self-modulation and by a small amount of dispersion. The signal $u_0(t)$ is an unchirped Gaussian pulse of initial RMS width $T_0 = 18$ ps transmitted through 40 km of NZ-DS fiber equivalent to $7.7 \times L_{NL}$ and $1.1 \times L_{D2}$, being $L_{NL} = (\gamma P_0)^{-1}$ the nonlinear distance and $L_{D2} = T_0^2/|\beta_2|$ the second-order dispersion length. The pulse was successfully recovered using the same value of Φ_{20}^r employed in the previous examples ($\Delta t / \Delta\omega = 21.9$ ps / ($2\pi 41.5$ GHz) = 84 ps^2), with SNR = 17 dB and a temporal intensity average of $N = 1000$. Again, we compare the RWT displays generated with three scaling parameters. The symmetric RWT display that is produced from the recovered pulse (see Fig. 5(a)) allows the more direct comparison of the RWT's profiles of the highest values, as it was done in Sec. 4. Figure 5(b) presents the peak values of the FRT irradiances for each fractional order p, when the scaling parameter σ_0 is –0.2, –0.3 and –0.4 ps^2/(nm·rad) in solid, dashed and dotted line, respectively. As it was previously discussed, the variation of the scaling factor produces a rearrangement of the RWT modifying, not only the value of the fractional order p_C where the maximum compression effect is observed, but the compression factor as well. The temporal intensities corresponding to the selected pulses from the RWT's generated with the three scaling parameters are shown in Fig. 5(c). The maximum compression effect is observed for the p_C values of 0.88, 0.83 and 0.77, when the scaling factor is –0.2, –0.3 and –0.4 ps^2/(nm·rad), respectively. The highest of these pulses is the one produced when σ_0 is the smallest in magnitude. To synthesize this pulse ($p_C = 0.88$) the associated device parameters become $\phi_{20} = -1.68\times10^{22}$ Hz^2 and $\Phi_{20} = -48.5$ ps^2 (or $L \cong 2.35$ km of standard optical fiber or an equivalent LCFG). The RF signal necessary to obtain the modulation parameter must be a cosine of amplitude $\theta_0 = 5$ rad and frequency $f_m = 9.22$ GHz, in phase with the pulse.

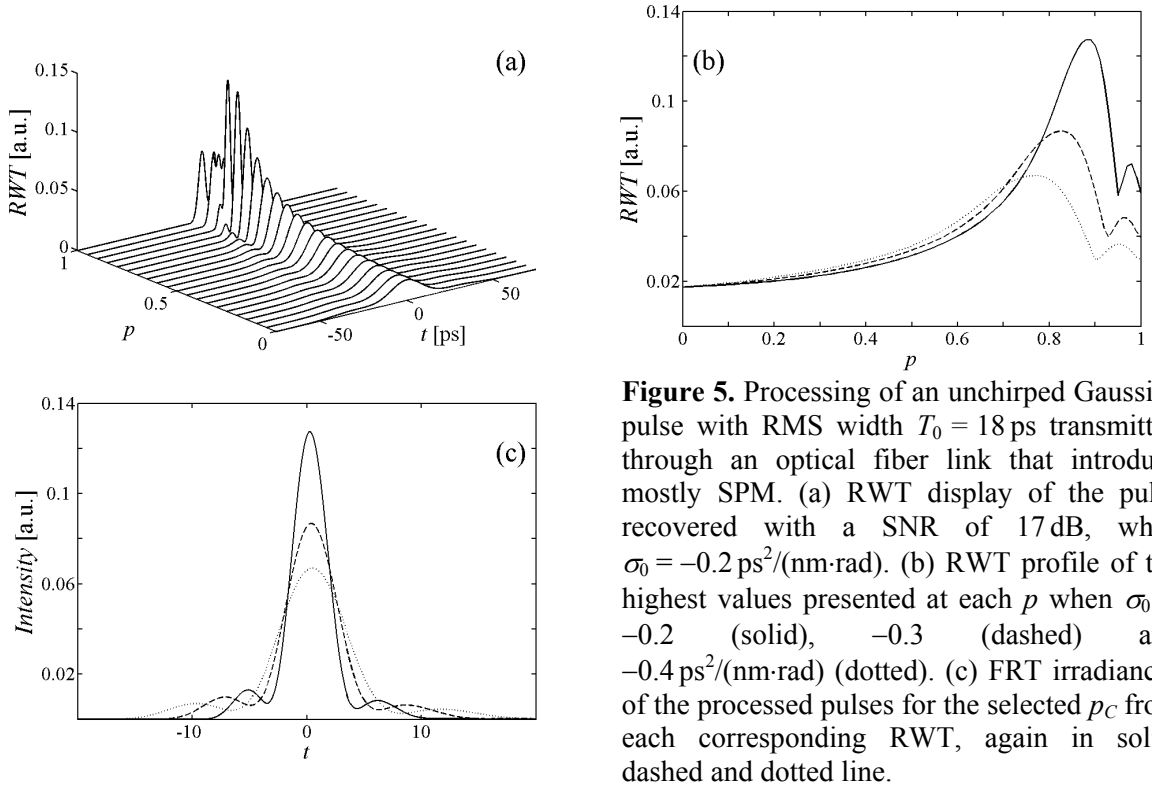

Figure 5. Processing of an unchirped Gaussian pulse with RMS width $T_0 = 18$ ps transmitted through an optical fiber link that introduce mostly SPM. (a) RWT display of the pulse recovered with a SNR of 17 dB, when $\sigma_0 = -0.2$ ps^2/(nm·rad). (b) RWT profile of the highest values presented at each p when σ_0 is –0.2 (solid), –0.3 (dashed) and –0.4 ps^2/(nm·rad) (dotted). (c) FRT irradiances of the processed pulses for the selected p_C from each corresponding RWT, again in solid, dashed and dotted line.

6. Conclusion

The temporal RWT was employed for pulse processing applications. Although the FRT irradiance can be obtained by properly combining electro-optic phase modulation and dispersive transmission, from a

practical point of view the signal analysis requiring a multiple, continuous production of the FRT (since p varies between 0 and 1) should be computationally produced. In this way the input signal to be processed should be known, which is not the case for most applications. To solve this problem, we applied a signal recovery method based on the recordings of two temporal intensities when the pulse has propagated through two media having second order dispersion of opposite signs. An upper bound limit for the second order dispersion value needed to appropriately obtain the phase of the pulse was given. Once the amplitude and phase information is recovered, the complete RWT for $0 < p < 1$ can be numerically produced. From this RWT display the adequate value of p required to process the pulse can be obtained. When the proper fractional order has been chosen, the synthesis operation of the pulse can be implemented by the use of a quadratic phase modulator in tandem with a LCFG. The practical realization of such a device involves a scaling factor that depends on the modulation and dispersive parameters. Variations of this factor produce changes in the RWT displays, which can yield an enhancement of the sought characteristic of the processed pulse. However, there is a practical limit for the scaling factor value imposed by the device parameters. We illustrated the method with applications concerning with pulse transmission by an optics fiber link affected with source chirping, third-order dispersion and self-phase modulation. Although most of the examples shown were focused on pulse compression, depending on the type of pulse and its Fourier transform, a symmetrizing operation can be readily performed. The effect of the detection noise was taken into account. It was noted, that the recovered pulse needs to be processed before generating the RWT, to reduce the noise floor introduced by the temporal intensity average done in the recording process. By windowing the pulse, the RWT analysis could be extended to cases with lower SNR, especially when the processing conditions correspond to fractional orders above ~0.7.

Acknowledgments
This work was supported by Consejo Nacional de Investigaciones Científicas y Técnicas (CONICET-PIP 112-200801-01769), Facultad de Ingeniería de la Universidad Nacional de La Plata (UNLP, Project I128), and Agencia Nacional de Promoción Científica y Tecnológica (ANPCyT, PICT 2005 38289). Laureano A. Bulus-Rossini is fellow of CONICET.

References
[1] Kolner B H and Nazarathy M 1989 *Opt. Lett.* **14** 630-632
[2] Papoulis A 1994 *J. Opt. Soc. Am.* A **11** 3-13
[3] van Howe J and Xu C 2006 *J. Lightwave Technol.* **24** 2649-2662
[4] Azaña J and Muriel M A 2000 *J. Quantum Electron.* **36** 517-526
[5] Azaña J and Muriel M A 2001 *J. Sel. Top. Quantum Electron.* **7** 728-744
[6] Berger N K, Levit B, Bekker A and Fischer B 2004 *Photon. Technol. Lett.* **16** 1855-1857
[7] Costanzo-Caso P A, Cuadrado-Laborde C, Duchowicz R and Sicre E E 2008 *Opt. Commun.* **281** 4001-4007
[8] Cuadrado-Laborde C, Costanzo-Caso P A, Duchowicz R and Sicre E E 2007 *Opt. Commun.* **275** 94-103
[9] Chantada L, Fernández-Pousa C R and Gómez-Reino C 2006 *J. Lightwave Technol.* **24** 2015-2025
[10] Lancis J, Caraquitena J, Andrés P and Muriel M A 2005 *Opt. Commun.* **253** 156-163
[11] Torres-Company V, Fernández-Pousa C R and Chen L R 2009 *Opt. Lett.* **34** 1885-1887
[12] Ozaktas H M, Zalevsky Z and Kutay M A 2001 *The Fractional Fourier Transform with Applications in Optics and Signal Processing* (Chichester: John Wiley & Sons)
[13] Lohmann A W 1993 *J. Opt. Soc. Am.* A **10** 2181-2186
[14] Ozaktas H M, Barshan B, Mendlovic D and Onural L 1994 *J. Opt. Soc. Am.* A **11** 547-559
[15] Lohmann A W and Soffer B H 1994 *J. Opt. Soc. Am.* A **11** 1798-1801
[16] Lohmann A W and Mendlovic D 1994 *Appl. Opt.* **33** 7661-7664

[17] Dorrer C and Walmsley I A 2005 *EURASIP J. Appl. Signal Processing* **10** 1541-1553
[18] Brunel M, Coetmellec S, Lelek M and Louradour F 2007 *J. Opt. Soc. Am.* A **24** 1641-1646
[19] Dragoman D and Dragoman M 1998 *Opt. Commun.* **145** 33-37
[20] Kane D J and Trebino R 1993 *J. Quantum Electron.* **29** 571-579
[21] Beck M, Raymer M G, Walmsley I A and Wong V 1993 *Opt. Lett.* **18** 2041-2043
[22] Iaconis C and Walmsley I A 1998 *Opt. Lett.* **23** 792-794
[23] Koumans R G M P and Yariv A 2000 *J. Quantum Electron.* **36** 137-144
[24] Dorrer C and Kang I 2003 *Opt. Lett.* **28** 1481-1483
[25] Dorrer C 2005 *Opt. Lett.* **30** 3237-3239
[26] Bulus-Rossini L A, Costanzo-Caso P A, Duchowicz R and Sicre E E 2010 *Opt. Commun.* **283** 2529-2535